ChemComm

Accepted Manuscript

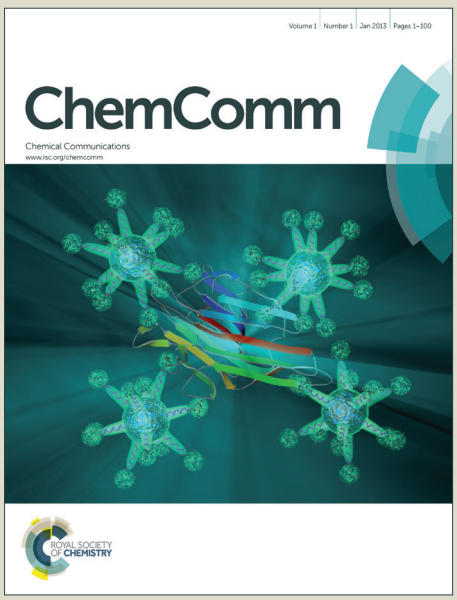

ROYAL SOCIETY OF CHEMISTRY

www.rsc.org/chemcomm

Cite this: DOI: 10.1039/c0xx00000x

www.rsc.org/xxxxxx

ARTICLE TYPE

In situ Assembly of Well-dispersed Gold Nanoparticles on Hierarchical Double-Walled Nickel Silicate Hollow Nanofibers as An Efficient and Reusable Hydrogenation Catalyst

Renxi Jin,[a] Yang Yang,[a] Yunfeng Li,[a] Lin Fang,[a] Yan Xing*[a] and Shuyan Song*[b]

Received (in XXX, XXX) XthXXXXXXXXX 20XX, Accepted Xth XXXXXXXXX 20XX
DOI: 10.1039/b000000x

Highly dispersive and ultrafine Au nanoparticles were effectively immobilized on the surface of hierarchical double-walled nickel silicate hollow nanofibers assembled by ultrathin nanosheets, which showed remarkable catalytic performances as an efficient and reusable hydrogenation catalyst.

In the field of nanoscience and nanotechnology, much emphasis has been placed on the catalysis of Au nanoparticles (AuNPs) since scientists discovered that AuNPs could be used as the catalysts for CO oxidation and the selective catalysis of acetylene hydrochlorination.[1] Compared with other metal catalysts (Pt, Pd, Cu, *etc*.), AuNPs have the highest selectivity and are less prone to metal leaching, over-oxidation, and self-poisoning, which enables them to be effective catalysts in a variety of catalytic reactions, such as selective oxidations, hydrogenations of organic compounds and selective NO_x reduction, *etc*.[2] However, as a soft metal, a potential issue of the ultrafine AuNPs lies in that they aggregate very easily and thus lose their activities. An efficient way to overcome the above problem is to anchor AuNPs onto a suitable support.[3] As an excellent Au-based catalyst, the following features are essential: a high specific surface area for dispersing AuNPs and effective contacting between reagents and AuNPs, an excellent stability and flexibility for resisting external stimuli and easy separation for reuse.[4] Research revealed that one-dimensional (1D) fibrous catalysts with high length-to-diameter ratio could be easily separated from fluid by sedimentation.[5] However, it is still necessary to develop methods or supports for anchoring ultrafine AuNPs on a hollow nanofibrous support with a high specific surface area and to prevent AuNPs aggregating under strong external stimuli.

Electrospinning has been exploited for many years as a remarkably simple and versatile technique to process polymer, carbon and metal oxides materials into 1D fibers.[6] By using this method, 1D hollow fibers could also be fabricated with multi-fluidic compound-jet or nonequilibrium heat-treatment.[7] However, the striking feature for most of these hollow fibers is that the walls of the fibers are generally composed of or aggregated from numerous simple nanoparticles with an irregular arrangement, which make them lack a high surface area, excellent stability and flexibility. Hierarchical self-assembly of nanosheets into novel architectures of higher dimensionality, especially multilevel hollow fibers, can help to enhance the performance as an easily recycled support. The flexible nanosheets can be spontaneously adjusted for better fixation of nanoparticles to prevent the aggregation of NPs and enhance the stability by the synergistic effect of the multilevel walls and hierarchical structure while maintaining a high specific surface area.[4c, 8] Thus, the fabrication of ultrafine and dispersive Au-based hollow fibrous nanocatalysts with a hierarchical multilevel structure assembled by ultrathin nanosheets is highly desired in catalysis.

Herein, we demonstrate a facile route to construct 1D nanofibrous catalysts with ultrafine AuNPs anchoring on the hierarchical double-walled nickel silicate hollow nanofibers (NSHNFs). As illustrated in Scheme 1, uniform silica hollow nanofibers (SHNFs) prepared using a facile single capillary electrospinning method are employed as the precursor. Then, the double-walled NSHNFs assembled by ultrathin nanosheets are synthesized using a simple hydrothermal treatment based on a SHNFs sacrificial templating process. Finally, the ultrathin AuNPs with well-dispersed distributions are anchored on the surface of ultrathin nanosheets of NSHNFs through a low-energy-consuming *in situ* reduction method. In this way, nanocomposites with Au nanoparticles immobilized on the hierarchical double-walled nickel silicate hollow nanofibers (AuNPs/NSHNFs) are formed and connected to form a network structure. The as-prepared AuNPs/NSHNFs show high catalytic activity and excellent stability as a remarkable catalyst due to their unique structures.

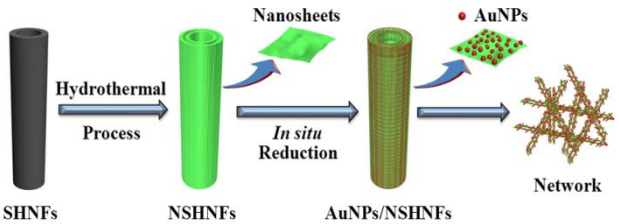

Scheme1. Schematic diagram of the formation of AuNPs/NSHNFs.

The SHNFs were fabricated *via* a facile single capillary electrospinning technique followed by calcination at 550 °C. As shown in Fig. S1, the electrospun SiO_2 nanofibers have a typical hollow structure with a relatively smooth surface and are connected to form network structure. After the hydrothermal

treatment in alkaline solution containing nickel ions at 100 °C for 10h, unique hierarchical hollow fibers with a high length-to-diameter ratio were obtained. The X-ray diffraction (XRD) pattern of the obtained fibers shows characteristic broad diffraction peaks that can be indexed to the nickel silicate ($Ni_3Si_4O_{10}(OH)_2 \cdot 5H_2O$, JCPDS card No. 43-0664) (Fig. S2).[9] The SEM image (Fig. 1a) shows that the obtained NSHNFs remain a network structure and the diameters of these fibers are 400-600 nm. However, the surface of the fibers was no longer smooth. From the magnified SEM image of the NSHNFs as shown in Fig. 1b and Fig. S3, the double-walled structure, the hollow interior, and the small primary units can be clearly discerned. TEM further confirms the double-walled structure of the as-synthesized NSHNFs. As can be seen from Fig. 1c, clear gaps between the outer and inner walls and the hollow interior can be observed. A magnified TEM image (Fig. 1d) clearly reveals that the walls of the as-prepared NSHNFs are composed of numerous ultrathin nanosheets. Meanwhile, the slight curl and self-attachment of the nanosheets result in the highly open and stable structure. Fig. S4 displays the N_2 adsorption desorption isotherm for the obtained NSHNFs. The BET surface area and total pore volume of the NSHNFs are 373 $m^2 g^{-1}$ and 0.41 $cm^3 g^{-1}$, respectively. The one-dimensional nanofibrous morphology, high length-to-diameter ratio, unique hierarchical double-walled hollow structure, small nanosheet units, large surface area make our sample probably be a high-performance catalyst support.

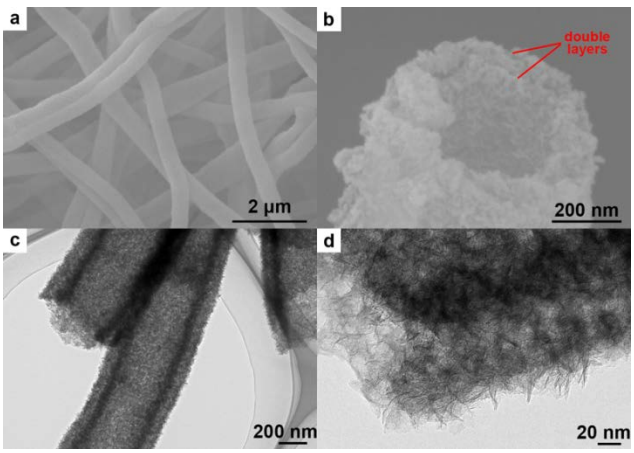

Fig. 1Typical FESEM (a, b) and TEM (c, d) images of NSHNFs.

The ultrafine and dispersive Au nanoparticle-nickel silicate hierarchical double-walled hollow nanofibers (AuNPs/NSHNFs) were fabricated *via* a simple and low-energy-consuming approach. First, the obtained NSHNFs with abundant hydroxy groups were activated in a $SnCl_2$ solution.[10] During this process, the Sn^{2+} was linked to the surface of NSHNFs through inorganic grafting. After tetrachloroauric acid ($HAuCl_4$) was added to the solution at room temperature, the linked Sn^{2+} species acted as a reducing agent to reduce Au^{3+} *in situ* on the surface of NSHNFs, because the standard reduction potential of the Sn^{4+}/Sn^{2+} (0.151 V *vs.* redox pair the standard hydrogen electrode, SHE) is lower than that of Au^{3+}/Au (1.52 V *vs.* SHE).[5a] Thus the AuNPs/NSHNFs were obtained. Meanwhile, their color gradually turned from pastel green to vermilion. The UV-Vis absorption spectra of aqueous suspensions of NSHNFs and AuNPs/NSHNFs were carried out. As observed in Fig. S5, a surface plasmon absorption band centered at around 525 nm appears on the absorption spectrum of aqueous suspensions of AuNPs/NSHNFs, which also indicates that the ultrafine AuNPs had been loaded on the surface of NSHNFs.

The AuNPs/NSHNFs were observed using transmission electron microscopy (TEM), and the corresponding results are shown in Fig. 2. Fig. 2a shows that the hierarchical double-walled nanofibrous structures assembled by nanosheets are maintained during the loading of the AuNPs. The magnified TEM image (Fig. 2b) clearly shows that the ultrafine AuNPs with well-dispersed distribution are uniformly located on the surfaces of ultrathin nanosheets and no large irregular Au particle is found. The size distribution histogram of AuNPs calculated from the corresponding TEM image is given in Fig. 2c. The particle size of AuNPs is 2.6 ± 0.5 nm. High-resolution TEM (HRTEM) image (Fig. 2d) shows that the estimated interplanar distance of the nanoparticles is approximately 0.23 nm, which corresponds well with the lattice spacing of the (111) plane of Au. Fig. S6 shows the XPS spectrum in Au 4f region of the as-prepared AuNPs/NSHNFs. It can be seen from the spectrum that the determined binding energy of Au $4f_{7/2}$ and Au $4f_{5/2}$ is 84.3 and 88.1 eV, respectively. The spin energy separation of the 4f doublet is 3.8 eV, indicating the metallic nature of gold (Au^0).[11] The energy-dispersive X-ray (EDX) spectrum from the corresponding TEM image confirms that the above AuNPs/NSHNFs are composed of Ni, Si, O, Sn, and Au element (Fig. S7).

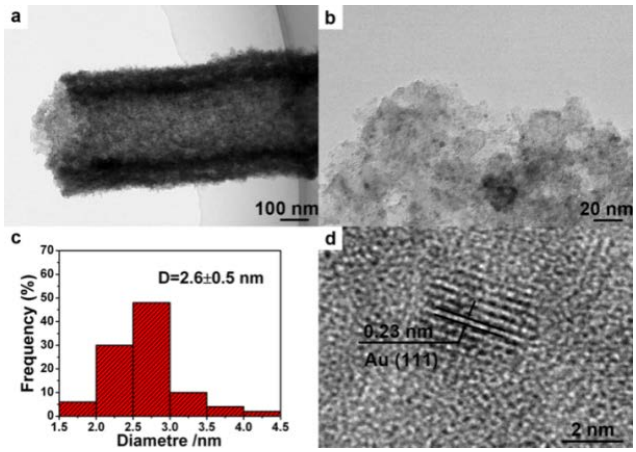

Fig. 2 Typical TEM images of AuNPs/NSHNFs (a, b); c) The size distribution histogram of AuNPs calculated from the corresponding TEM image; d) An HRTEM image of the AuNP.

A high dispersion of ultrafine AuNPs on NSHNFs can be useful for many potential applications. Here, we selected the reduction of 4-nitrophenol (4-NP) to 4-aminophenol (4-AP) by $NaBH_4$ asmodel system to evaluate the catalytic hydrogenation performance of AuNPs/NSHNFs.[12] Upon the addition of $NaBH_4$, the absorption peak shifts from 317 to 400 nm owing to the formation of 4-nitrophenolate ions (Fig. S8a). When a trace amount of AuNPs/NSHNFs (1 mg) are added, the absorption at 400 nm decreases immediately with a concomitant increase in the

peak of 4-AP at 295 nm with time. As observed in Fig. 3a, the time for the complete reduction of 4-NP over AuNPs/NSHNFs is about 280 s. However, no reaction is happened even for 2.5 h in a control experiment when pure NSHNFs or Sn^{2+}/NSHNFs being used as the catalyst (Fig. S8b). Since the amount of $NaBH_4$ is in large excess (C($NaBH_4$)/C(4-NP) = 100 : 1), pseudo-first-order kinetics could be applied for the evaluation of rate constant.[13] Fig. 3b displays the linear relationship between ln (C/C_0) and reaction time in the reaction and the corresponding rate constant k is calculated to be 12.01 × 10^{-3} s^{-1}. Turnover frequency (TOF), defined as the number of moles of reduced 4-NP per mole surface Au atoms per hour when the conversion has reached 90%, is calculated to further investigate the efficiency of the AuNPs/NSHNFs. The TOF of the as-prepared AuNPs/NSHNFs (the theoretical loading amount of AuNPs of 3 wt% is considered) can reach 298 h^{-1}, which is higher than other substrate-supported Au nanocatalysts reported in most previous studies (Table S1). The high catalytic activity of AuNPs/NSHNFs is attributed to their unique hierarchical double-walled hollow structure assembled by ultrathin nanosheets and the highly dispersed and ultrafine AuNPs. The double hollow interiors, ultrathin nanosheet units, large surface area and highly dispersive AuNPs allow the effective contact between the 4-NP and AuNPs in the reaction. The ultrafine AuNPs on the NSHNFs make a large potential difference, thus leading to a high rate of reduction.

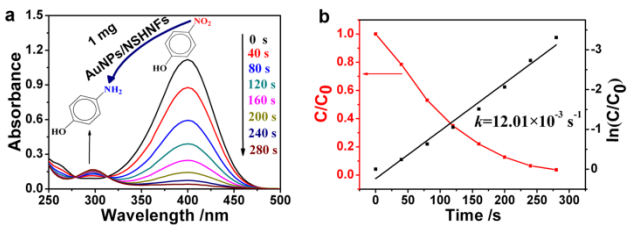

Fig. 3 a) UV-Vis absorption spectra during the catalytic reduction of 4-NP over AuNPs/NSHNFs; b) The black and red squares are the ln(C/C_0) and C/C_0 *versus* reaction time for the reduction of 4-NP over AuNPs/NSHNFs, respectively. C_0 and C is the absorption peak at 400 nm initially and at time t.

Stability is also one of the most important factors in the practical applications of nanocatalysts. Here, we firstly investigated the cyclic stability of AuNPs/NSHNFs by reusing the catalyst four cycles. As shown in Fig. S9, the catalytic activity of AuNPs/NSHNFs remains almost unchanged after four cycles. Fig. S10 shows that the morphology of NSHNFs are retained and AuNPs are remained dispersed quite well on the surface of NSHNFs following the reduction reaction, which is vital for high catalytic activity, even after being recycled for several times. In addition, we also heated the as-prepared AuNPs/NSHNFs at 500 °C for 2h to investigate their thermostability. As shown in Fig. S11, the AuNPs on the surface of nanosheets maintain their dispersed state without obvious aggregation, which indicates that the AuNPs/NSHNFs have good thermal stability and resistance to sintering. The following factors may contribute to the excellent stability of the AuNPs/NSHNFs: (1) The AuNPs/NSHNFs could be recovered easily by sedimentation due to the high length-to-diameter ratio of the NSHNFs; (2) The flexible nanosheets upon adsorption of AuNPs facilitate the fixation of AuNPs on the surface and prevent AuNPs agglomeration under the external stimulus; (3) The strong affinity between the AuNPs and NSHNFs *via* this synthesis method prevents the AuNPs dropping out of the NSHNFs.

In conclusion, we have demonstrated an effective route to the synthesis of nanofibrous nanocomposites composed of highly dispersive and ultrafine AuNPs immobilized on hierarchical double-walled nickel silicate hollow nanofibers assembled by ultrathin nanosheets. The nanosheet-composed unique structure played a significant role in the nanocatalyst system for high catalytic activity and excellent stability during the catalytic process. Due to facile synthesis and excellent catalytic performance of Au supported hierarchical double-walled hollow nanofibrous silicate materials, it could possibly inspire future research in preparation of highly efficient catalysts for practical catalytic applications.

This work is supported by the National Natural Science Foundation of China (Grant No. 21073032); Research Fund for the Doctoral Program of Higher Education of China (No. 20120043110005); The project development plan of science and technology of Jilin Province (No. 20140101110JC); Opening Fund of State Key Laboratory of Rare Earth Resource Utilization, Changchun Institute of Applied Chemistry, Chinese Academy of Sciences; Opening Fund of State Key Laboratory of Inorganic Synthesis and Preparative Chemistry of Jilin University.

Notes and references

[a] *College of Chemistry, Northeast Normal University, Changchun, 130024, China; E-mail: xingy202@nenu.edu.cn; Tel: +86-431-85099657.*
[b] *State Key Laboratory of Rare Earth Resource Utilization, Changchun Institute of Applied Chemistry, Chinese Academy of Sciences, Changchun, 130012, China; E-mail: songsy@ciac.ac.cn.*

† Electronic Supplementary Information (ESI) available: See DOI: 10.1039/b000000x/

1 (a) G. J. Hutchings, *J. Catal.*, 1985, **96**, 292; (b) M. Haruta, T. Kobayashi, H. Sano and N. Yamada, *Chem.Lett.*, 1987, 405.
2 (a) S. Carrettin, J. Guzman and A. Corma, *Angew. Chem. Int. Ed.*, 2005, **44**, 2242; (b) F. Boccuzzi, A. Chiorino, M. Manzoli, D. Andreeva,T. Tabakova, L. Ilieva and V. Iadakiev, *Catal. Today*, 2002,**75**, 169; (c) A. S. Hashmi and M. Rudolph, *Chem. Soc. Rev.*, 2008, **37**, 1766; (d) A. S. Hashmi and G. J. Hutchings, *Angew. Chem. Int. Ed.*, 2006, **45**, 7896; (e) M. Rudolph and A. S. Hashmi, *Chem. Soc. Rev.*, 2012, **41**, 2448; (f) J. Huang, Y. Zhu, M. Lin, Q. Wang, L. Zhao, Y. Yang, K. X. Yao and Y. Han, *J. Am. Chem. Soc.*, 2013, **135**, 8552.
3 (a) L. S. Zhong, J. S. Hu, Z. M. Cui, L. J. Wan, and W. G. Song, *Chem.Mater.*, 2007, **19**, 4557; (b) L. You, Y. W. Mao and J. P. Ge, *J. Phys. Chem. C*, 2012, **116**, 10753-; (c) Y. Chi, L. Zhao, Q. Yuan, X. Yan, Y. J. Li, N. Li and X. T. Li, *J. Mater. Chem.*, 2012, **22**, 13571; (d) T. Ishida and M. Haruta, *Angew. Chem. Int. Ed.*, 2007, **46**, 7154.
4 (a) Q. L. Fang, S. H. Xuan, W. Q. Jiang and X. L. Gong, *Adv. Funct. Mater.*, 2011, **21**, 1902; (b) S. Xuan, W. Jiang and X. Gong, *Dalton Trans.*, 2011, **40**, 7827; (c) Q. Ji, J. P. Hill and K. Ariga, *J. Mate. Chem. A*, 2013, **1**, 3600.
5 (a) Z. Zhang, C. Shao, P. Zou, P. Zhang, M. Zhang, J. Mu, Z. Guo, X. Li, C. Wang and Y. Liu, *Chem. Commun.*, 2011, **47**, 3906; (b) Z. Y. Zhang, C. L. Shao, Y. Y. Sun, J. B. Mu, M. Y. Zhang, P. Zhang, Z. C. Guo, P. P. Liang, C. H. Wang and Y. C. Liu, *J. Mater. Chem.*, 2012, **22**, 1387; (c) P. Zhang, C. Shao, Z. Zhang, M. Zhang, J. Mu, Z. Guo and Y. Liu, *Nanoscale*, 2011, **3**, 3357.
6 (a) S. Cavaliere, S. Subianto, I. Savych, D. J. Jones and J. Roziere, *Energy Environ. Sci.*, 2011, **4**, 4761; (b) V. Kalra, J. H. Lee, J. H. Park, M. Marquez and Y. L. Joo, *Small*, 2009, **5**, 2323; (c) X. F. Wang, B. Ding, J. Y. Yu and M. R. Wang, *Nano Today*, 2011, **6**, 510.

7 (a) Y. Zhao, X. Cao, L. Jiang, *J. Am. Chem. Soc.*, 2007, **129**, 764; (b) H. Chen, N. Wang, J. Di, Y. Zhao, Y. Song and L. Jiang, *Langmuir*, 2010, **26**, 11291; (c) F. Mou, J. G. Guan, W. Shi, Z. Sun and S. Wang, *Langmuir*, 2010, **26**, 15580.

8 (a) B. Liu, S. Wei, Y. Xing, D. Liu, Z. Shi, X. Liu, X. Sun, S. Hou and Z. Su, *Chem. Eur. J.*, 2010, **16**, 6625; (b) Q. Ji, C. Guo, X. Yu, C. J. Ochs, J. P. Hill, F. Caruso, H. Nakazawa and K. Ariga, *Small*, 2012, **8**, 2345; (c) R. Jin, Y. Xing, X. Yu, S. Sun, D. Yu, F. Wang, W. Wu and S. Song, *Chem. Asian J.*, 2012, **7**, 2955.

9 Y. Wang, C. Tang, Q. Deng, C. Liang, D. H. Ng, F. L. Kwong, H. Wang, W. Cai, L. Zhang and G. Wang, *Langmuir*, 2010, **26**, 14830.

10 N. Takahashi and K. Kuroda, *J. Mater. C.*, 2011, **21**, 14336.

11 (a) L. Tan, D. Chen, H. Liu and F. Tang, *Adv. Mater.*, 2010, **22**, 4885; (b) M. P. Casaletto, A. Longo, A. Martorana, A. Prestianni and A. M. Venezia, *Surf. Interface Anal.*, 2006, **38**, 215.

12 (a) J. Ge, Q. Zhang, T. Zhang and Y. Yin, *Angew. Chem. Int. Ed.*, 2008, **47**, 8924-8928; (b) S. H. Wu, C. T. Tseng, Y. S. Lin, C. H. Lin, Y. Hung and C. Y. Mou, *J. Mater. Chem.*, 2011, **21**, 789.

13 J. Zeng, Q. Zhang, J. Chen and Y. Xia, *Nano Lett.*, 2010, **10**, 30.